Triplex DNA Clamp Regulates Cas12a Activation for ssDNA and RNA Sensing

Andrea Celeste Di Pede[#], Neda Bagheri[#], Erica Belforte[#], Alessio Palone[#], Marianna Rossetti,[#] and Alessandro Porchetta[#,*]

Department of Chemical Science and Technologies, University of Rome, Tor Vergata, Via della Ricerca Scientifica 1, 00133 Rome, Italy

Keywords: CRISPR sensor, Clamp-like binding, Triplex DNA, trans-cleavage activity, Cas12a,

Abstract

We present a molecular strategy that enables the programmable activation of CRISPR-Cas12a system in response to Triplex DNA formation triggered by single stranded DNA (ssDNA) or RNA inputs. This assay, called Triplex Regulated Activation of Cas12a for ssDNA and RNA sensing (TRACR), leverages the highly specificity of clamp-like triplex structures to control a strand displacement mechanism within a rationally designed DNA hairpin (PAM-Switch). Upon displacement and PAM complementation, the Cas12a ribonucleoprotein (RNP) is activated, initiating *trans*-cleavage and producing a concentration-dependent fluorescent signal. By decoupling target recognition (via triplex formation) from direct hybridization with the Cas12a-crRNA complex, TRACR eliminates the need for target-specific crRNAs. This design also allows multiple, spatially resolved detection of distinct nucleic acid targets within a single Cas12a reaction. Through the use of triplex-based clamps, TRACR achieves high specificity for single-nucleotide variants and supports the detection of both ssDNA and RNA targets across a broad range of lengths (10–20 nucleotides). TRACR addresses key limitations in current Cas12-based diagnostics and opens new avenues for nucleic acid sensing.

Introduction

Clustered regularly interspaced short palindromic repeats (CRISPR)-based toolbox aims to create the next generation of *in vitro* molecular diagnostics for routine clinical use. Since the discovery of the collateral (i.e. *trans*-) cleavage activity of RNA and single stranded DNA (ssDNA) by CRISPR-Cas type V and VI systems, a variety of biomolecular sensors and assays have been reported for molecular diagnostics.(1–6) Among them, platforms based on the RNA-programmed Cas12 effector have gained particular interest as Cas12 contains a single RuvC nuclease domain that cleaves complementary double-stranded DNA (dsDNA) adjacent to a T-rich protospacer adjacent motif (PAM) and ssDNA nonspecifically (*trans*-cleavage).(7,8) Despite significant advancements towards applications outside research lab, Cas12a-based molecular assays still faces limitations. First, *trans*-cleavage is activated by base-pairing of a nucleic acid target to a complementary crRNA guide.(9) This requirement imposes the use of a specific ribonucleoprotein (RNP) complex for each DNA target thus preventing easy multiplexing and increasing the cost of screening analysis. Second, its natural dsDNA-targeting activity has limited its application for RNA detection.(10–12) On this respect, recently, a split-activator highly accessible RNA analysis (SAHARA) strategy using short RNA inputs has been reported showing RNA substrates activating *trans*-cleavage activity of Cas12a.(13) However, the approach still requires the hybridization between a starter DNA and a crRNA guide (e.g., at least 16 base pairs).(13) Third, Cas12a systems tolerates some mismatches between the crRNA and the target DNA to prevent immune evasion,(14) and so the specificity varies depending on the position and number of the mismatch (MM) (15,16). This leads to limited detection specificity for single base mutations,(1,15–17) posing challenges for the identification of disease-related point mutations.(18) In particular, the specificity of Cas12a detection system is slightly higher for dsDNA targets but is limited for single base mismatches in ssDNA targets.(19) Therefore, developing molecular strategies to enhance CRISPR specificity is essential to expanding its applicability.

To enhance specificity and better transduce chemical information into biochemical functions, Nature often employs binding-induced conformational change mechanisms(20–22). In particular, clamp-like structure switching mechanism using two recognition elements to embrace a single copy of target molecule results in enhanced binding affinity with superior specificity for biomolecule detection. (23–26) As an example, molecular chaperones employ clamp-like binding sites to protect unstable protein conformers (due to the larger recognition interface) and guide their transition to the native state.(27) Ring-shaped DNA sliding clamps also take advantage of a clamp-like binding mechanism to control DNA replication and genome maintenance.(28) These observations have inspired the design of clamp-like switches for artificial biotechnologies in the areas of biomolecular sensing and imaging.(29–33) Among them, synthetic clamp-like DNA probes have been used to achieve precise control over specific functions in response to external inputs, especially when designed to be controlled by allosteric effectors.(34–37) A simple approach for engineering a clamp-

like DNA binding mechanism is through Triplex DNA, which integrates Hoogsteen interactions with Watson-Creek-Franklin base pairing.(30) Triplex switches can be designed to undergo conformational changes that enable the binding of nucleic acid targets and the formation of a parallel triple-helix.(38–42) Specifically, the non-canonical DNA triplex structure consists of a polypurine/polypyrimidine duplex, with a third strand binding the major groove via Hoogsteen pairing and aligning parallel to the purine-rich strand. In this configuration, thymine pairs with A-T (TAT triplets), while protonated cytosine pairs with G-C (CG-C^+ triplets) through Hoogsteen hydrogen bonds.(43–45) The clamp-like structure offers key advantages, including pH-responsive triplex formation due to Hoogsteen interactions.(46,47) Additionally, the two-step clamp-like triplex folding improves target specificity and binding affinity,(23,25,26,30) yielding enhanced target discrimination compared to duplex-based detection systems.(30,48) These features have led to the application of clamp-like DNA Triplexes in gene regulation,(46,47) nanomedicine,(49,50) smart drug delivery systems.(51,52)

Building on these findings, we present here a Triplex-regulated strategy to precisely control Cas12a activity (TRACR) for molecular sensing applications. TRACR leverages the high specificity of clamp-like DNA Triplex for DNA/RNA target recognition in combination with a PAM-engineered DNA hairpin (PAM-Switch) to activate Cas12a *trans*- cleavage.(53) Central to this design is a triplex-controlled toehold strand displacement reaction which induces a hairpin-to-duplex reconfiguration of the PAM-Switch. This mechanism effectively decouples target recognition (via triplex formation) from hybridization with the Cas12a ribonucleoprotein (RNP) complex.(54) By employing a clamp-like binding mechanism, our system enhances specificity for single-base mutation detection and enables the detection of both ssDNA and RNA targets across a wide range of lenghts (from 10 to 20 nt). In addition, TRACR supports spatially resolved detection of distinct NA targets within a single CRISPR reaction mix. By combining triplex-based recognition with programmable strand displacement, this platform addresses key limitations of current CRISPR-sensing platforms.

Results and Discussion

Design of Triplex-controlled CRISPR-Cas12a system

Our design involves two DNA modules engineered to trigger Cas12a activity only in the presence of a specific nucleic acid (NA) input: (1) a Clamp-Switch DNA probe for the recognition of the NA target of interest which folds into a Triplex DNA only upon target binding (Triplex Clamp, Figure 1A), and (2) a specifically designed PAM-engineered DNA switch (i.e. PAM-Switch) that activates CRISPR-Cas12a only upon hairpin to duplex reconfiguration and PAM complementation. To monitor downstream collateral cleavage activity, a Cas12a reaction mix including the ribonucleoprotein (RNP) complex and a FRET-based DNA reporter is added in solution (Fig. 1A and B). The Clamp-Switch probe is composed of different functional motifs. Its core consists of two polypyrimidine portions (orange motifs, Figure 1B): the first one recognizes the polypurine

ssDNA/RNA target through Watson-Crick-Franklin (W-C-F) interactions (dashed lines), while the second one binds to duplex DNA via parallel Hoogsteen interactions (dotted lines) through a clamp-like switching mechanism. Thus, the formation of the Triplex Clamp is driven by structure-switching mechanism, resulting in Clamp-Switch closure exclusively in the presence of the NA target (Figure S1A). These two polypyrimidine motifs are separated by a flexible, unstructured 4-base loop and are flanked by two tail regions (indicated as a, b and c) that are complementary to the corresponding motifs (a*, b* and c*) of the PAM-Switch.

The second module consists of a DNA hairpin (PAM-Switch), in which the anti-PAM sequence (PAM*) is sequestered within a short loop connecting two self-complementary DNA domains targeted by Cas12a. This configuration includes a 20-base pair stem formed by the hybridization of two complementary strands: the target strand (TS) and the non-target strand (NTS), designated as domains a and a*, respectively (Figure 1B). In its folded hairpin conformation, the PAM site remains inaccessible, thereby maintaining the Cas12a activity in an inactive state. We have recently demonstrated that by employing an optimized PAM-Switch design, it is possible to control Cas12a activation in response to external molecular cues as a means of hairpin-to-duplex reconfiguration.(53)

Here, we take advantage of the proximity effect of the Triplex Clamp's flanking portions (orange motifs, Figure 1B) induced by target binding to trigger a toehold strand displacement reaction (SDR) on the PAM-Switch. The SDR is associated with a hairpin-to-duplex conformational change which exposes the PAM motif, enabling Cas12a binding and activity. Specifically, a toehold motif of Clamp-Switch (c, light blue) complementary with the toehold region of the PAM-Switch probe is necessary to drive the SDR (c*, light blue). Upon triplex formation, a displacement domain (b, dark green, and a, red) of the Clamp-Switch complements the 20-base Cas12 targeting region of the PAM-Switch (b*, dark green) and the locked PAM* sequence (a*, red) (Figure 1B). As a result, folded Triplex Clamp probe induce the reconfiguration of the PAM-Switch and activates Cas12a, generating a concentration-dependent *trans*-cleavage activity (Figure 1B).

Notably, the NA target (orange strand, Figure 1B) does not interact directly with the crRNA guide of the RNP complex but is instead recognized by the clamp region of the Clamp-Switch probe (c, orange portion in Figure 1B), offering several advantages. First, it allows Cas12a activation in response to any triplex-forming NA sequence, eliminating the need for ssDNA sequence complementarity with the crRNA. In principle, our modular design may help achieve the detection of multiple targets using a single CRISPR reaction mixture.(55) By modifying the clamp region of the triplex probe - without the need to redesign the crRNA guide for each target - the system eliminates the need of different crRNAs, thereby ensuring optimal *trans*- cleavage for any target.(56) Secondly, the clamp-like triplex formation enhances binding affinity due to Hoogsteen interactions (Figure S1). Finally, the triplex structure provides a dual mechanism for target recognition which results in increased specificity to single base mutations compared to duplex DNA.(30)

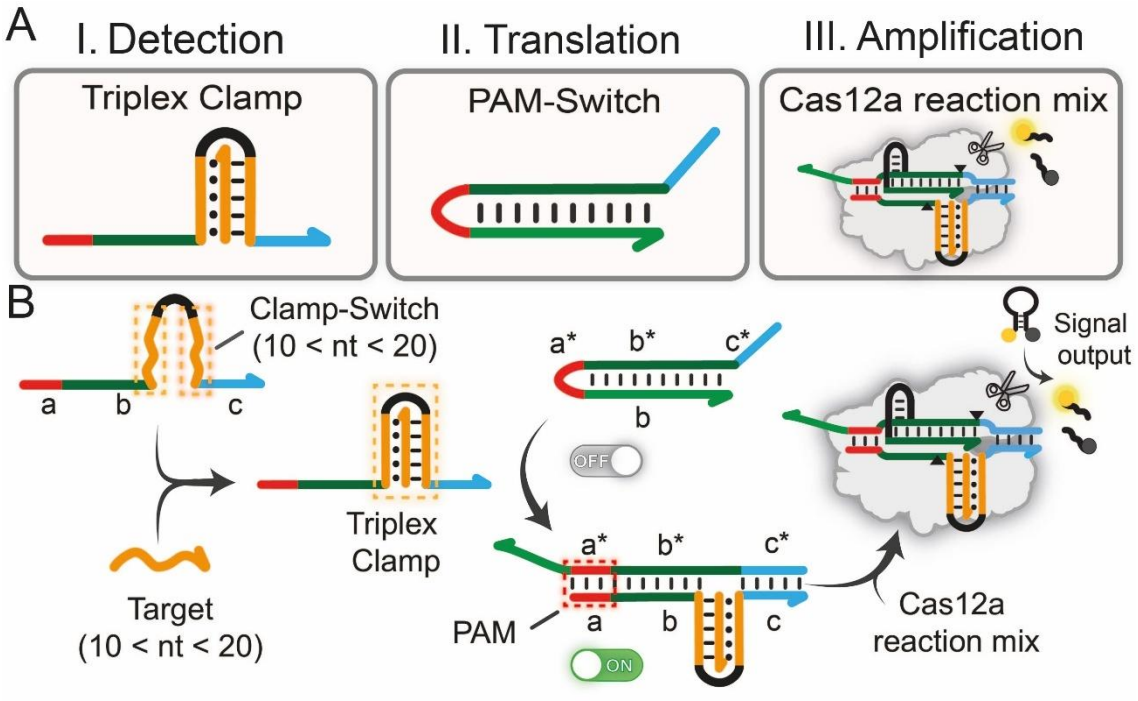

Figure 1. Design of TRACR system for sensing applications. (**A**) Schematic representation of the three functional modules required to activate the detection system. (**B**) Clamp-Switch adopts its folded triplex conformation only in the presence of a homopurine ssDNA/RNA target in solution. Target binding induces the formation of the Triplex Clamp which subsequently triggers the hairpin strand displacement reaction. This reaction induces hairpin-to-duplex conformational change of the PAM-Switch module and PAM complementation, enabling Cas12a activation of the *trans*-cleavage activity and consequent generation of fluorescence output.

Hairpin Strand Displacement Reaction (SDR) Controlled by Triplex Clamp Formation

Toehold and displacement domains can function independently or in combination,(57,58) and the introduction of an unstructured loop between them can hinder the strand displacement reaction on the time scale of analysis.(59,60) Our design leverages the key concept that target-induced triplex formation brings the toehold and displacement domains into close proximity, inducing strand invasion and hairpin-to-duplex reconfiguration of PAM-Switch (Figure 2A). To demonstrate this, we monitored this reaction using a Cas12a reaction mix (RNP 20 nM, FRET-based DNA reporter 100 nM) in the presence and absence of the T14 ssDNA target (Figure 2B). As expected, we observe a concentration-dependent signal increase only when T14 is added in solution, as a consequence of triplex-driven strand displacement reaction, PAM complementation and subsequent Cas12a activation (Figure S2). We performed different control experiments to confirm the proposed mechanism. First, Triplex Clamp formation was studied using a Clamp-Switch (CS_FQ) with a 20 nt clamp region on each side modified with a fluorophore-quencher pair (FAM-BHQ1) at the termini of the clamp region. Binding assays with ssDNA targets of different lengths (from 10 to 20 nt) confirmed the triplex formation (Figure S3). Of note, as Hoogsteen

interactions (both CG-C⁺ triplets and TA-T triplets) are sensitive to pH changes, also the observed binding affinity is pH-dependent ($K_{D,\ pH\ 6.5}$ = 2 ± 1 nM, $K_{D,pH\ 7.0}$ = 5 ± 1 nM, $K_{D,pH\ 7.5}$ = 51 ± 7 nM, $K_{D,pH\ 8.0}$ = 265 ± 1 nM, see Figure S4). To confirm that the hairpin-to-duplex transition of the PAM-Switch probe depends only on triplex formation, we monitored toehold-mediated strand displacement reaction using a fluorophore (FAM)-tagged PAM-Switch (PAM-Switch_F) and a BHQ1-labelled Clamp-Switch probe (CS_Q). As expected, fluorescence quenching is observed only in response to hairpin-to-duplex switch, showing a kinetic profile consistent with that associated with a linear invading strand (Figure S5). For further optimization, we tested Clamp-Switch probes with different numbers of 5'- extra bases and varying toehold lengths (0, 6, 12 and 18 nt, Figure S6). (57) Extra 5'-terminal nucleotides on the Clamp-Switch facilitate efficient hairpin-to-duplex transition as expected by the thermodynamics of hairpin strand displacement reactions. As expected, CRISPR-powered strand displacement controlled by triplex formation exhibits higher sensitivity (LOD = 0.3 nM), enabling detection of target concentrations one order of magnitude lower than that obtained with the hybridization-based hairpin strand displacement reaction without amplification. Of note, the pM sensitivity aligns with that reported for pre-amplification free Cas12-based assays.(61,62) The kinetics profiles of SDRs, however, show slightly slower signal generation over time as a consequence of the time required to enable molecular reconfiguration of the probes and Cas12 binding/activation.

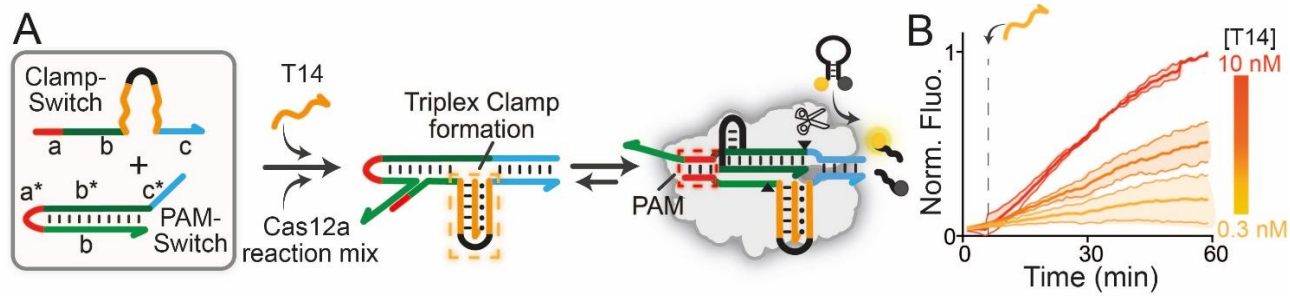

Figure 2. (**A**) Schematic representation of Triplex-based SDR downstream controlling Cas12 activity. The formation of the Triplex Clamp triggers the strand displacement and enables PAM complementation (indicated in red), thereby activating Cas12a binding and *trans*-cleavage activity. (**B**) Kinetic profiles showing ssDNA detection when the reaction is combined with downstream Cas12a-based signal amplification. The Cas12a-based triplex SDR was conducted by adding different concentration of T14 (0.3 – 1 – 10 nM) to a solution containing PAM-Switch (0.5 nM), Clamp-Switch (CS_14, 20 nM), and a Cas12a reaction mixture (20 nM RNP complex and 100 nM FRET-based DNA reporter). All experiments were carried out in 10 mM Tris-HCl buffer (pH 7.0), containing 10 mM $MgCl_2$ and 50 mM NaCl at 37 °C.

Optimization of Triplex-based Cas12 assay for ssDNA detection

To optimize our detection system, we used a ssDNA Target of 14nt as model target (T14, see Table 3 in the SI). Of note, Cas12a detection system requires DNA targets of at least 16 nt in length for the direct activation of collateral cleavage activity.(1) Here, we aim to demonstrate that also shorter ssDNA can be used to control Cas12a detection systems (Figure 3A). To demonstrate this, we first optimized the Cas12-based assay conditions in terms of PAM-Switch (0.5 nM) and Clamp-Switch (20 nM) concentrations (Figure S7 and S8). Under such experimental conditions, a

rapid activation of the Cas12a detection system is observed over time in response to the addition of increasing concentrations of T14 (Figure 3B) and picomolar sensitivity (LOD: 791 pM, Figure 3C). Then, we performed specificity tests using variant sequences of T14 having a single base mutation at different positions. Of note, affinity-based binding assays using a fluorophore-quencher Clamp-Switch (CS_FQ) confirmed that Triplex Clamp formation is highly specific for single base mutations (Figure S9A). Since pH strongly affects Hoogsteen interactions and triple helix stability, the specificity can be easily tuned by changing the pH of the solution (Figure S9B). To investigate the overall specificity of the Triplex-based Cas12a detection system, we tested three different pH values (pH 7.0, 7.5, and 7.9). Our data reflect the pH-dependent folding of Triplex Clamp showing a different detection specificity when the Triplex Clamp folding is integrated into the CRISPR-Cas12a recognition system (Figure 3D). Specifically, we observe an increased specificity at higher pH values (7.5 and 7.9), consistent with the lower stability of the Triplex Clamp structure under mildly alkaline conditions. This behavior reflects the intrinsic characteristics of triplex DNA, where even a single-base mismatch can substantially impair triplex formation - an effect that is more pronounced at higher pH values due to the reduced protonation of cytosines required for stable CG-C^+ triplet interactions. The reduced protonation weakens hydrogen bonding, destabilizing the triplex structure. As a result, the combination of mismatch-induced destabilization and pH-dependent triplex dissociation synergistically enhances the system's capacity to discriminate single-nucleotide variants (SNVs) at slightly alkaline pH values.(63) To demonstrate this, we performed specificity assays by screening ssDNA targets containing either C (i.e. MM_C variants) or T (MM_T variants) mismatches at each position along the T14 sequence, confirming high specificity for the tested targets. As expected, a central mismatch in the triplex destabilizes the formation of the triple helix more than the presence of the mutation in the terminal positions of the sequence (Figure 3E). In addition, a G→C substitution results in a further enhancement of specificity compared to an A→T substitution (Figure S10).

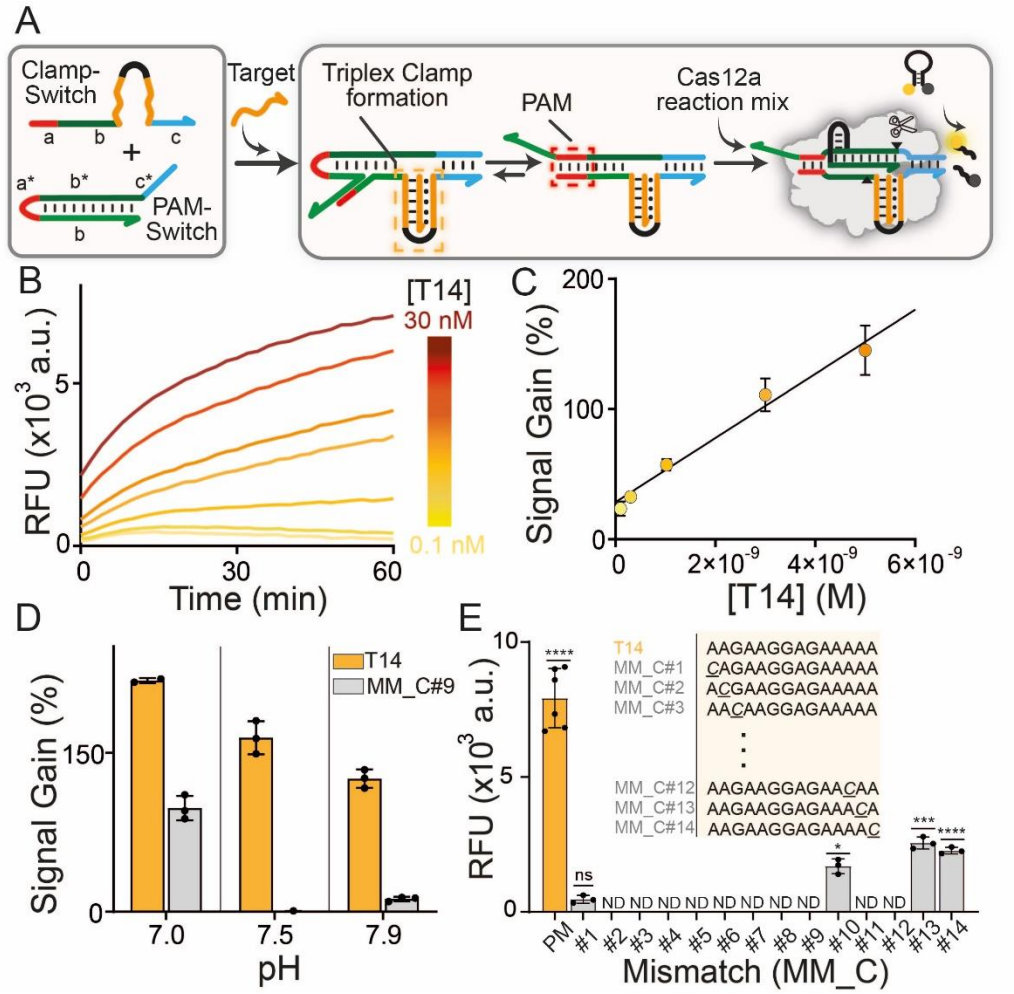

Figure 3. Proof-of-concept demonstration of highly specific Cas12a-powered detection of ssDNA using Triplex Clamp structure. (**A**) Schematic representation of the triplex-based Cas12a detection system. (**B**) Time-dependent fluorescence kinetic analysis showing the detection of increasing concentrations (0.1 nM, 0.3 nM, 1 nM, 3 nM, 5 nM, 10 nM, 30 nM) of T14. (**C**) Linear dynamic range (between 0.1 and 5 nM; R^2 = 0.9522, n = 3) of T14 concentration obtained by plotting fluorescence signal change versus target concentration. Signal gain values (%) were calculated after 15 min of cleavage activity and represent the relative fluorescence signal change associated with collateral cleavage activity due to the addition of T14. (**D**) Specificity study performed at three different pH values using 5 nM of a single-nucleotide mismatch (MM#9) and T14 perfect match. Signal gain values (%) were calculated after 15 min cleavage reaction. All the values reported show the mean ± SD, where n = 3 replicates. (**E**) Bar graphs showing the difference between the fold change with respect to the perfect match (T14) (5 nM) and to the specific single-nucleotide mismatch (MM_C) target (5 nM). All the values reported show the mean ± SD, where n = 3 replicates. Comparisons of the different signal output between PM and MM with the control (in the absence of the ssDNA target) were performed using an unpaired t-test with Welch's correction (n = 3). The asterisks denote values levels of statistical significance: P< 0.0001 (****); P< 0.001 (***); P< 0.001 (**); P ≤ 0.005 (*).

Triplex-controlled Cas12a detection regulated by ssDNA and RNA targets of different lengths

To generalize the approach, we tested the platform using ssDNA targets of varying lengths by simply changing the clamp portion of the Clamp-Switch DNA responsible for target recognition (Figure 4A, see Table 2 and 3). Kinetic fluorescence analysis demonstrates that our triplex-based platform enables the detection of homopurine ssDNA targets of different lengths (from 12 to 20 nt)

(Figure 4B). We also performed specificity assays using mutated variants (i.e. C-type point mutations in the middle of the sequence) by collecting the signal of the perfect match target (PM, 10 nM) and the corresponding signal of mutated target (MM, 10 nM) at pH values comprised between pH 7.0 and 7.9 confirming enhanced detection specificity under slightly alkaline pH values for all the ssDNA target lengths tested (Figure 4C). Notably, the specificity improves as the length decreases, as a single base mutation has higher impact on the overall free energy of triplex folding. To further generalize the proposed method, we also demonstrated the possibility of combining our triplex-based hybridization network with an isothermal pre-amplification step to achieve ultrasensitive detection using nicking enzyme-assisted amplification (LOD = 10 fM, Figure S11). Of note, this isothermal DNA amplification generates ssDNA amplicon and thus can be easily combined with our triplex-based detection systems.

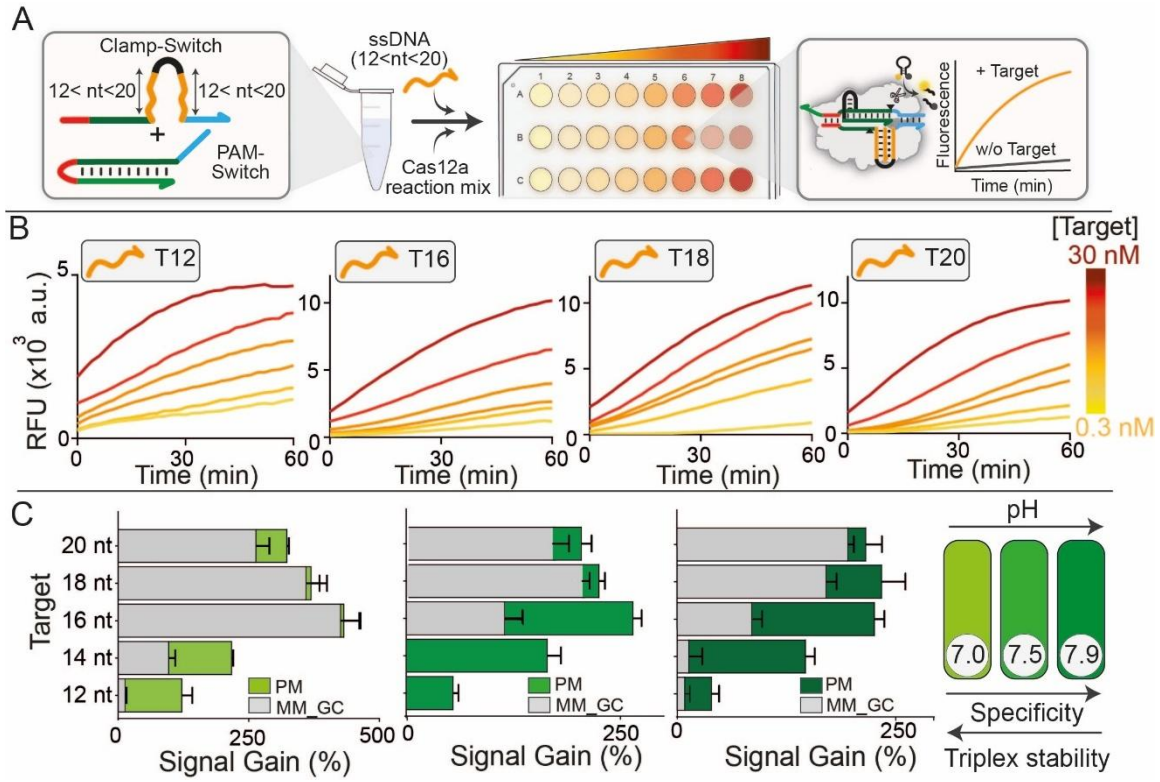

Figure 4. (**A**) Schematic description of the proposed triplex-based CRISPR assay for the detection of ssDNA targets of different lengths (from 12 nt to 20 nt) by simply changing the Clamp-Switch probe using the same Cas12a reaction mix. (**B**) Time-dependent fluorescence kinetic analysis of Cas12a collateral cleavage at increasing concentrations of ssDNA targets. The experiments were conducted by adding different concentrations of ssDNA target (0.3 nM, 1 nM, 3 nM, 5 nM, 10 nM, 30 nM) to a solution containing PAM-Switch (0.5 nM) and 20 nM of the specific Clamp-Switch (see Table 2), and incubating at 37 °C for 15 min. These solutions were then mixed with the Cas12a reaction mix (RNP complex 20 nM, FRET-based DNA reporter 100 nM) previously incubated at 37 °C for 30 min. All the experiments were conducted in a buffer containing 10 mM Tris-HCl, 50 mM NaCl, 10 mM $MgCl_2$, pH 7.0. (**C**) Superimposed bar graphs show the fluorescence signal intensities generated by perfect match (PM) and single-nucleotide mismatch (MM_GC) targets (5 nM, measured at t = 15 min) under three different pH conditions (pH 7.0, 7.4, and 7.9, from left to right). For each condition, 10 nM of single-stranded DNA target (PM or MM; see Table 3) was introduced into a solution containing 0.5 nM PAM-Switch and 20 nM Clamp-Switch. Separately, the Cas12a reaction mixture (20 nM ribonucleoprotein (RNP) complex and 100 nM FRET-based DNA reporter) was preincubated at 37 °C for 30 minutes and subsequently added to the target-containing

solutions. Reactions were carried out in buffer containing 10 mM Tris-HCl, 50 mM NaCl, and 10 mM $MgCl_2$. Fluorescence values represent the mean ± standard deviation (SD) of three independent replicates (n = 3).

Additionally, we have also adapted the design for the detection of RNA targets. It is well-established that Cas12a can naturally recognize and discriminate dsDNA targets, making its adaptation for RNA detection challenging. To achieve this goal, we modified the clamp region of the Clamp-Switch probe (see Figure 1, orange portions) generating a hybrid RNA-DNA Clamp-Switch probe (CS_RNA) that features the two clamp regions made of RNA. The hybrid RNA-DNA probe is necessary because enable the triplex formation, whereas DNA-based clamp-like probes cannot fold into triplex structure in the presence of RNA targets.(39) By doing so, we are able to detect RNA targets of various lengths (10 to 20 nt) with a sensitivity in the picomolar range (Figure 5).

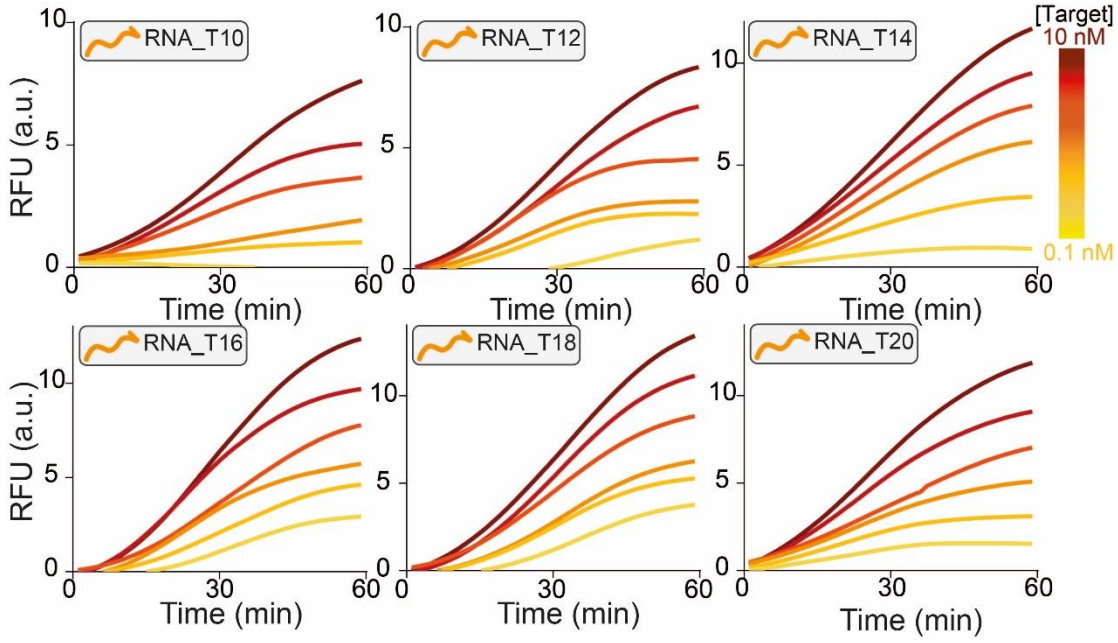

Figure 5. Kinetic profiles of the RNA Triplex-based activation of Cas12a detection system. Experiments were performed at 37 °C to evaluate RNA targets of different lengths (from 10 nt to 20 nt) at increasing concentrations (0.1, 0.3, 1, 3, 5, and 10 nM). RNA targets were introduced into a reaction buffer solution containing 10 mM Tris-HCl, 50 mM NaCl, and 10 mM $MgCl_2$ (pH 7.0), supplemented with 0.5 nM PAM-SW and 20 nM CS_ RNA. Following a 15-min incubation at 37 °C, a Cas12a reaction mixture (FRET-based DNA reporter 100 nM + RNP complex 20 nM) was added and fluorescence signal acquisition was started immediately.

"Well-resolved" ssDNA target detection using a single Cas12-based reaction mix in an array-based fluorescence platform

Since our strategy does not require modification of the RNP complex to recognize different nucleic acid (NA) targets, we further investigated the potential for parallel NA analysis using a single Cas12a reaction mix. As a proof-of-concept demonstration, we designed two additional Clamp-Switch probes (designated V2 and V3), each containing a unique clamp motif (purple for V2

and blue for V3; Figure 6A) that selectively binds to its corresponding ssDNA target. Notably, the target sequences for V2 and V3 (T14_V2 and T14_V3; see Table 2) consist of scrambled homopurine sequences that ensure orthogonality. Each of the three ssDNA targets (T14, T14_V2, and T14_V3) was successfully detected using the same RNP complex thanks to the specificity of the corresponding Clamp-Switch modules (Figure 6A, right; Figure S12). To assess the system's ability to discriminate between targets, we implemented a spatially resolved detection format using standard 96-well plates (25 µL per well), where each well contained a specific Clamp-Switch probe. The resulting heatmap demonstrates the system's capacity to detect and distinguish each target with high specificity and without significant cross-reactivity (Figure 6B). When only one ssDNA target is present in the reaction mix, fluorescence can be observed exclusively in the well containing the matching Clamp-Switch probe. When multiple targets are mixed, the spatial distribution of fluorescence allowed unambiguous identification of each individual ssDNA species. This setup enables parallel screening of multiple nucleic acid targets with a single, unmodified Cas12a reaction mix without the need for target-specific RNPs. Importantly, signal intensities and response times remained consistent and robust even in the presence of non-cognate targets, highlighting the scalability and efficiency of this compartmentalized detection approach for nucleic acid sensing.

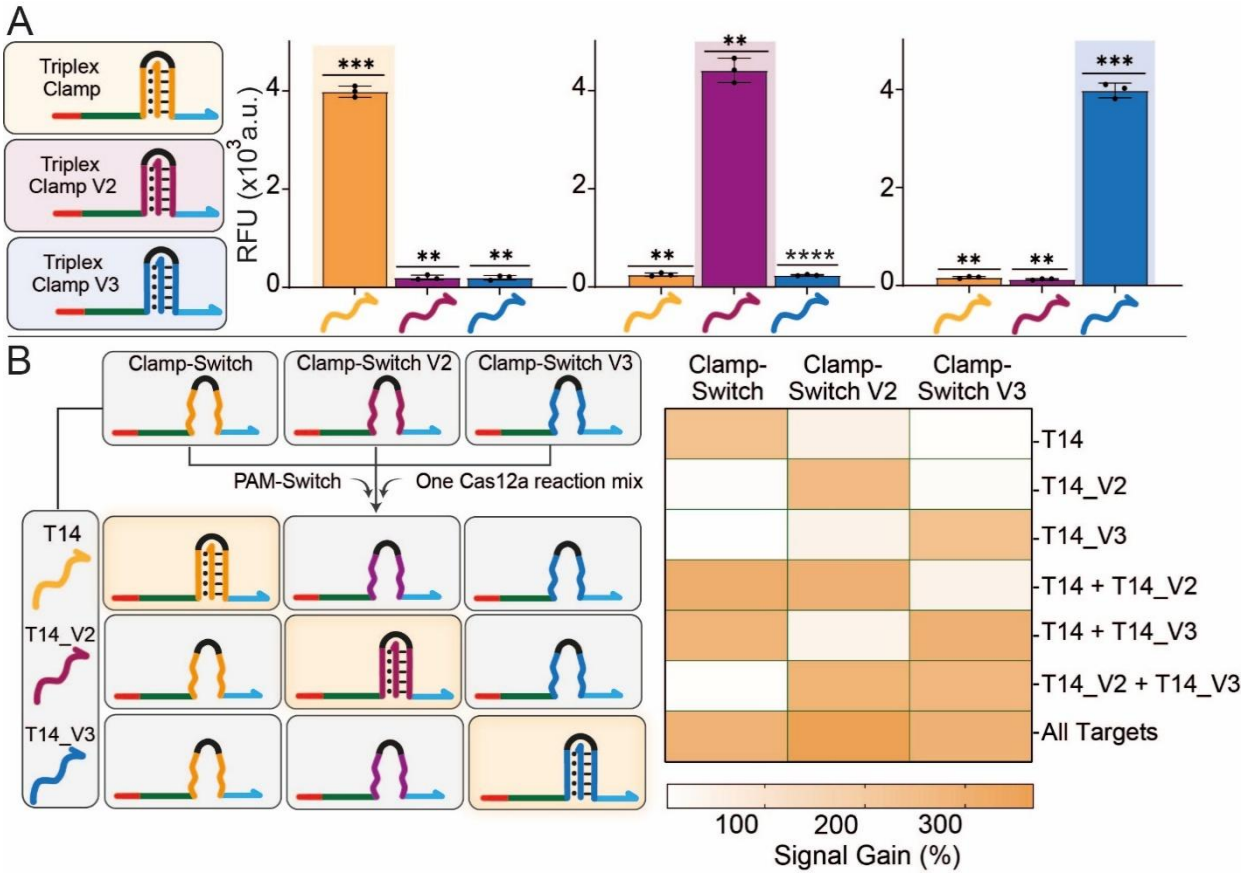

Figure 6. Spatially resolved detection of distinct ssDNA targets using a well-array platform. (**A**) Bar graph depicting the sequence-dependent and highly specific interactions between various ssDNA targets and their corresponding clamp domains, leading to the activation of Cas12a collateral cleavage activity. Probe complementarity is

highlighted using matched color coding. Experiments were conducted at 37 °C by adding a CRISPR-Cas12a reaction mix (20 nM RNP complex and 100 nM FRET-based DNA reporter) to a buffer containing 10 mM Tris-HCl, 50 mM NaCl and 10 mM $MgCl_2$ (pH 7.0), supplemented with PAM-Switch (0.5 nM), the corresponding Clamp-Switch (20 nM), and ssDNA targets (T14, T14_V2, T14_V3; 5 nM each), pre-incubated at 37 °C for 15 min. The reported Relative Fluorescence Units (RFU) were measured after 15 min of reaction and represent the change in fluorescence signal induced by Cas12a trans-cleavage in the presence and absence of the ssDNA target. Data are expressed as mean ± standard deviation (SD), n = 3 replicates. Statistical analysis was performed using a two-tailed unpaired t-test with Welch's correction. Significance levels are indicated as follows: ****P < 0.0001; ***P < 0.001; **P < 0.01; *P ≤ 0.05. (**B**) Schematic overview of the experimental workflow (left) and bar graph (right) showing the Signal Gain (%) of Triplex-based Clamp-Switch modules in response to different combinations of the three ssDNA targets (see Methods in Supporting Information for details). Signal Gain (%) was calculated after 15 minutes of cleavage reaction. Values are reported as mean ± SD, n = 3 replicates.

Conclusions

In this study, we report a strategy to control CRISPR-Cas12a activation through a nucleic acid-based hybridization network triggered by clamp-like formation of a triplex DNA. Specifically, we show that Cas12a activity can be modulated via a triplex-based strand displacement system that drives the conformational change of a PAM-Switch probe from a hairpin to a duplex state. This transition enables PAM complementation and consequent Cas12a activation. TRACR enables Cas12a activation without requiring complementarity between the crRNA sequence and the target nucleic acid, allowing the use of a single ribonucleoprotein (RNP) complex for the detection of multiple distinct oligonucleotide sequences. We show that it is possible to detect multiple ssDNA and RNA targets, achieving picomolar sensitivity using the same Cas12a RNP complex. TRACR is flexible as it expands detection to oligonucleotides shorter than those typically required for direct Cas12a-based activation (15-16 nt). Furthermore, by using a Clamp-Switch probe as target recognition module, TRACR also overcome one of the major limitations of standard Cas12a diagnostics — namely, the difficulty in discriminating single-nucleotide variants (SNVs). Our system enables precise discrimination between mismatched (MM) and perfectly matched (PM) sequences, thanks to the enhanced selectivity of the triplex-forming Clamp-Switch probe.

Despite these promising results, specific limitations of the method should be highlighted. TRACR relies on the presence of homopurine sequences in the target nucleic acid that support triple helix formation. While such homopurine-rich regions are found in various bacterial and viral genomes, this structural requirement inevitably restricts the range of sequences that can be targeted and may limit the assay's universality. Nevertheless, the platform's inherent orthogonality, along with its capacity to detect different target lengths - including those below the length threshold typically required for Cas12a activation – offers a significant advantage. This enables the simultaneous detection of multiple distinct motifs within the same gene, even in the presence of closely related sequences, thus expanding the diagnostic potential. Importantly, TRACR introduces a versatile molecular engineering strategy to address several of the intrinsic challenges associated with Cas12a-based sensing. By integrating structure switching via programmable triplex formation

induced by nucleic acid inputs, the system achieves enhanced sequence specificity, increased tolerance to short targets, and modular multiplexing capabilities. Taken together, these features may broaden the scope of CRISPR-Cas12a applications in nucleic acid diagnostics—particularly in scenarios requiring single-nucleotide resolution, such as clinical diagnostics, pathogen detection, and precision medicine. Moreover, the conditional control strategy demonstrated here could be generalized to other CRISPR systems, paving the way for more adaptable and intelligent molecular tools in nanomedicine and synthetic biology.

References

1. Chen JS, Ma E, Harrington LB, Da Costa M, Tian X, Palefsky JM, et al. CRISPR-Cas12a target binding unleashes indiscriminate single-stranded DNase activity. Science. 2018 Apr;360(6387):436–9. doi: 10.1126/science.aar6245

2. Rossetti M, Merlo R, Bagheri N, Moscone D, Valenti A, Saha A, et al. Enhancement of CRISPR/Cas12a trans-cleavage activity using hairpin DNA reporters. Nucleic Acids Res. 2022 Aug;50(14):8377–91. doi: 10.1093/nar/gkac578

3. Li SY, Cheng QX, Wang JM, Li XY, Zhang ZL, Gao S, et al. CRISPR-Cas12a-assisted nucleic acid detection. Cell Discov. 2018 Apr;4(1):1–4. doi: 10.1038/s41421-018-0028-z

4. Aman R, Mahas A, Mahfouz M. Nucleic Acid Detection Using CRISPR/Cas Biosensing Technologies. ACS Synth Biol. 2020 Jun;9(6):1226–33. doi: 10.1021/acssynbio.9b00507

5. Kellner MJ, Koob JG, Gootenberg JS, Abudayyeh OO, Zhang F. SHERLOCK: nucleic acid detection with CRISPR nucleases. Nat Protoc. 2019 Oct;14(10):2986–3012. doi: 10.1038/s41596-019-0210-2

6. Cheng X, Li Y, Kou J, Liao D, Zhang W, Yin L, et al. Novel non-nucleic acid targets detection strategies based on CRISPR/Cas toolboxes: A review. Biosens Bioelectron. 2022 Nov;215:114559. doi: 10.1016/j.bios.2022.114559

7. Phan QA, Truong LB, Medina-Cruz D, Dincer C, Mostafavi E. CRISPR/Cas-powered nanobiosensors for diagnostics. Biosens Bioelectron. 2022 Feb;197:113732. doi: 10.1016/j.bios.2021.113732

8. Del Giovane S, Bagheri N, Di Pede AC, Chamorro A, Ranallo S, Migliorelli D, et al. Challenges and perspectives of CRISPR-based technology for diagnostic applications. TrAC Trends Anal Chem. 2024 Mar;172:117594. doi: 10.1016/j.trac.2024.117594

9. Creutzburg SC, Wu WY, Mohanraju P, Swartjes T, Alkan F, Gorodkin J, Staals RH, Van Der Oost J. Good guide, bad guide: spacer sequence-dependent cleavage efficiency of Cas12a. Nucleic acids research. 2020 Apr;48(6):3228-43. doi: 10.1093/nar/gkaa121

10. Aman R, Mahas A, Marsic T, Hassan N, Mahfouz MM. Efficient, rapid, and sensitive detection of plant RNA viruses with one-pot RT-RPA–CRISPR/Cas12a assay. Frontiers in microbiology. 2020 Dec;11:610872. doi: 10.3389/fmicb.2020.610872

11. Feng W, Peng H, Xu J, Liu Y, Pabbaraju K, Tipples G, et al. Integrating Reverse Transcription Recombinase Polymerase Amplification with CRISPR Technology for the One-Tube Assay of RNA. Anal Chem. 2021 Sep;93(37):12808–16. doi: 10.1021/acs.analchem.1c02292

12. Zhang WS, Pan J, Li F, Zhu M, Xu M, Zhu H, et al. Reverse Transcription Recombinase Polymerase Amplification Coupled with CRISPR-Cas12a for Facile and Highly Sensitive Colorimetric SARS-CoV-2 Detection. Anal Chem. 2021 Mar;93(8):4126–33. doi: 10.1021/acs.analchem.0c05080

13. Rananaware SR, Vesco EK, Shoemaker GM, Anekar SS, Sandoval LSW, Meister KS, et al. Programmable RNA detection with CRISPR-Cas12a. Nat Commun. 2023 Sep;14(1):5409. doi: 10.1038/s41467-023-41207-z

14. Schelling MA, Nguyen GT, Sashital DG. CRISPR-Cas effector specificity and cleavage site determine phage escape outcomes. PLoS Biol. 2023 Apr;21(4):e3002065. doi: 10.1371/journal.pbio.3002065

15. Murugan K, Seetharam AS, Severin AJ, Sashital DG. CRISPR-Cas12a has widespread off-target and dsDNA-nicking effects. J Biol Chem. 2020 Apr;295(17):5538–53. doi: 10.1074/jbc.RA119.011873

16. Strohkendl I, Saifuddin FA, Rybarski JR, Finkelstein IJ, Russell R. Kinetic Basis for DNA Target Specificity of CRISPR-Cas12a. Mol Cell. 2018 Sep;71(5):816-824.e3. doi: 10.1016/j.molcel.2018.07.032

17. Ai J, Deng J, Hu J, Pu X, Yuan T, Teng Y, et al. PAM-Independent CRISPR-Cas12a System for Specific Assays of Single Nucleotide Variants. JACS Au. 2025 Mar;5(3):1392–401. doi: 10.1021/jacsau.4c00678

18. Cohen JD, Li L, Wang Y, Thoburn C, Afsari B, Danilova L, et al. Detection and localization of surgically resectable cancers with a multi-analyte blood test. Science. 2018 Feb;359(6378):926–30. doi: 10.1126/science.aar3247

19. Li H, Cui X, Sun L, Deng X, Liu S, Zou X, et al. High concentration of Cas12a effector tolerates more mismatches on ssDNA. FASEB J. 2021;35(1):e21153. doi: 10.1096/fj.202001684R

20. Vogt AD, Di Cera E. Conformational Selection Is a Dominant Mechanism of Ligand Binding. Biochemistry. 2013 Aug;52(34):5723–9. doi: 10.1021/bi400750k

21. Csermely P, Palotai R, Nussinov R. Induced fit, conformational selection and independent dynamic segments: an extended view of binding events. Trends Biochem Sci. 2010 Oct;35(10):539–46. doi: 10.1016/j.tibs.2010.05.003

22. Weikl TR, Paul F. Conformational selection in protein binding and function. Protein Sci Publ Protein Soc. 2014 Nov;23(11):1508–18. doi: 10.1002/pro.2558

23. Vinkenborg JL, Nicolson TJ, Bellomo EA, Koay MS, Rutter GA, Merkx M. Genetically encoded FRET sensors to monitor intracellular Zn2+ homeostasis. Nat Methods. 2009 Oct;6(10):737–40. doi: 10.1038/nmeth.1373

24. Gerstein M, Krebs W. A database of macromolecular motions. Nucleic Acids Res. 1998 Sep;26(18):4280–90. doi: 10.1093/nar/26.18.4280

25. Stratton MM, Loh SN. Converting a protein into a switch for biosensing and functional regulation. Protein Sci. 2011;20(1):19–29. doi: 10.1002/pro.556

26. Herschlag D. The role of induced fit and conformational changes of enzymes in specificity and catalysis. Bioorganic Chem. 1988 Mar;16(1):62–96. doi: 10.1016/0045-2068(88)90009-0

27. Stirling PC, Bakhoum SF, Feigl AB, Leroux MR. Convergent evolution of clamp-like binding sites in diverse chaperones. Nat Struct Mol Biol. 2006 Oct;13(10):865–70. doi: 10.1038/nsmb1142

28. Xu ZQ, Jergic S, Lo ATY, Pradhan AC, Brown SHJ, Bouwer JC, et al. Structural characterisation of the complete cycle of sliding clamp loading in Escherichia coli. Nat Commun. 2024 Sep;15(1):8372. doi: 10.1038/s41467-024-44555-x

29. Bertucci A, Guo J, Oppmann N, Glab A, Ricci F, Caruso F, et al. Probing transcription factor binding activity and downstream gene silencing in living cells with a DNA nanoswitch. Nanoscale. 2018 Jan;10(4):2034–44. doi: 10.1039/C7NR07814E

30. Idili A, Plaxco KW, Vallée-Bélisle A, Ricci F. Thermodynamic Basis for Engineering High-Affinity, High-Specificity Binding-Induced DNA Clamp Nanoswitches. ACS Nano. 2013 Dec;7(12):10863–9. doi: 10.1021/nn404305e

31. Saunders J, Thompson IAP, Soh HT. Generalizable Molecular Switch Designs for In Vivo Continuous Biosensing. Acc Chem Res. 2025 Mar;58(5):703–13. doi: 10.1021/acs.accounts.4c00721

32. Idili A, Amodio A, Vidonis M, Feinberg-Somerson J, Castronovo M, Ricci F. Folding-Upon-Binding and Signal-On Electrochemical DNA Sensor with High Affinity and Specificity. Anal Chem. 2014 Sep;86(18):9013–9. doi: 10.1021/ac501418g

33. Rangel AE, Hariri AA, Eisenstein M, Soh HT. Engineering Aptamer Switches for Multifunctional Stimulus-Responsive Nanosystems. Adv Mater. 2020;32(50):2003704. doi: 10.1002/adma.202003704

34. Rossetti M, Ranallo S, Idili A, Palleschi G, Porchetta A, Ricci F. Allosteric DNA nanoswitches for controlled release of a molecular cargo triggered by biological inputs. Chem Sci. 2017 Jan;8(2):914–20. doi: 10.1039/C6SC03404G

35. Grosso ED, Idili A, Porchetta A, Ricci F. A modular clamp-like mechanism to regulate the activity of nucleic-acid target-responsive nanoswitches with external activators. Nanoscale. 2016 Oct;8(42):18057–61. doi: 10.1039/C6NR06026A

36. Farag N, Mattossovich R, Merlo R, Nierzwicki Ł, Palermo G, Porchetta A, et al. Folding-upon-Repair DNA Nanoswitches for Monitoring the Activity of DNA Repair Enzymes. Angew Chem Int Ed. 2021;60(13):7283–9. doi: 10.1002/anie.202016223

37. Hu Y, Wang Z, Chen Z, Pan L. Switching the activity of Taq polymerase using clamp-like triplex aptamer structure. Nucleic Acids Res. 2020 Sep;48(15):8591–600. doi: 10.1093/nar/gkaa634

38. Roberts RW, Crothers DM. Specificity and stringency in DNA triplex formation. Proc Natl Acad Sci. 1991 Nov;88(21):9397–401. doi: 10.1073/pnas.88.21.9397

39. Frank-Kamenetskii MD, Mirkin SM. TRIPLEX DNA STRUCTURES. Annu Rev Biochem. 1995 Jul;64(Volume 64, 1995):65–95. doi: 10.1146/annurev.bi.64.070195.000433

40. Liu CQ, Shi XF, Bai CL, Zhao J, Wang Y. Comparative Studies on Parallel and Antiparallel Duplex and Triplex DNA. J Theor Biol. 1997 Feb;184(3):319–26. doi: 10.1006/jtbi.1996.0267

41. Nadal A, Eritja R, Esteve T, Pla M. “Parallel” and “Antiparallel Tail-Clamps” Increase the Efficiency of Triplex Formation with Structured DNA and RNA Targets. ChemBioChem. 2005;6(6):1034–42. doi: 10.1002/cbic.200500117

42. Hu Y, Cecconello A, Idili A, Ricci F, Willner I. Triplex DNA Nanostructures: From Basic Properties to Applications. Angew Chem Int Ed. 2017;56(48):15210–33. doi: 10.1002/anie.201705266

43. Idili A, Vallée-Bélisle A, Ricci F. Programmable pH-Triggered DNA Nanoswitches. J Am Chem Soc. 2014 Apr;136(16):5836–9. doi: 10.1021/ja501782z

44. Chandrasekaran AR, Rusling DA. Triplex-forming oligonucleotides: a third strand for DNA nanotechnology. Nucleic Acids Res. 2018 Feb;46(3):1021–37. doi: 10.1093/nar/gkx1274

45. Thompson IAP, Zheng L, Eisenstein M, Soh HT. Rational design of aptamer switches with programmable pH response. Nat Commun. 2020 Jun;11(1):2946. doi: 10.1038/s41467-020-16688-5

46. Noonberg SB, Scott GK, Garovoy MR, Benz CC, Hunt CA. In vivo generation of highly abundant sequence-specific oligonucleotides for antisense and triplex gene regulation. Nucleic Acids Res. 1994 Jul;22(14):2830–6. doi: 10.1093/nar/22.14.2830

47. Zhou Z, Giles KE, Felsenfeld G. DNA·RNA triple helix formation can function as a cis-acting regulatory mechanism at the human β-globin locus. Proc Natl Acad Sci. 2019 Mar;116(13):6130–9. doi: 10.1073/pnas.1819837116

48. Iacovelli F, Idili A, Benincasa A, Mariottini D, Ottaviani A, Falconi M, et al. Simulative and Experimental Characterization of a pH-Dependent Clamp-like DNA Triple-Helix Nanoswitch. J Am Chem Soc. 2017 Apr;139(15):5321–9. doi: 10.1021/jacs.7b01101

49. Pei H, Zuo X, Zhu D, Huang Q, Fan C. Functional DNA Nanostructures for Theranostic Applications. Acc Chem Res. 2014 Feb;47(2):550–9. doi: 10.1021/ar400262r

50. Liu S, Jiang Q, Zhao X, Zhao R, Wang Y, Wang Y, et al. A DNA nanodevice-based vaccine for cancer immunotherapy. Nat Mater. 2021 Mar;20(3):421–30. doi: 10.1038/s41563-020-00887-0

51. Ren J, Hu Y, Lu CH, Guo W, Aleman-Garcia MA, Ricci F, et al. pH-responsive and switchable triplex-based DNA hydrogels. Chem Sci. 2015 Jun;6(7):4190–5. doi: 10.1039/C5SC01434A

52. Chen X, Chen T, Ren L, Chen G, Gao X, Li G, et al. Triplex DNA Nanoswitch for pH-Sensitive Release of Multiple Cancer Drugs. ACS Nano. 2019 Jun;13(6):7333–44. doi: 10.1021/acsnano.9b02805

53. Bagheri N, Chamorro A, Idili A, Porchetta A. PAM-Engineered Toehold Switches as Input-Responsive Activators of CRISPR-Cas12a for Sensing Applications. Angew Chem Int Ed. 2024;63(17):e202319677. doi: 10.1002/anie.202319677

54. Simmel FC, Yurke B, Singh HR. Principles and applications of nucleic acid strand displacement reactions. Chemical reviews. 2019 Feb;119(10):6326-69. doi: 10.1021/acs.chemrev.8b00580

55. Bruch R, Urban GA, Dincer C. CRISPR/Cas Powered Multiplexed Biosensing. Trends Biotechnol. 2019 Aug;37(8):791–2. doi: 10.1016/j.tibtech.2019.04.009

56. Creutzburg SCA, Wu WY, Mohanraju P, Swartjes T, Alkan F, Gorodkin J, et al. Good guide, bad guide: spacer sequence-dependent cleavage efficiency of Cas12a. Nucleic Acids Res. 2020 Apr;48(6):3228–43. doi: 10.1093/nar/gkaa121

57. Weng Z, Yu H, Luo W, Guo Y, Liu Q, Zhang L, et al. Cooperative Branch Migration: A Mechanism for Flexible Control of DNA Strand Displacement. ACS Nano. 2022 Feb;16(2):3135–44. doi: 10.1021/acsnano.1c10243

58. Xing Y, Yang Z, Liu D. A Responsive Hidden Toehold To Enable Controllable DNA Strand Displacement Reactions. Angew Chem Int Ed. 2011;50(50):11934–6. doi: 10.1002/anie.201105969

59. Ratajczyk EJ, Bath J, Šulc P, Doye JP, Louis AA, Turberfield AJ. Controlling DNA–RNA strand displacement kinetics with base distribution. Proceedings of the National Academy of Sciences. 2025 Jun;122(23):e2416988122. doi: 10.1073/pnas.2416988122

60. Machinek RRF, Ouldridge TE, Haley NEC, Bath J, Turberfield AJ. Programmable energy landscapes for kinetic control of DNA strand displacement. Nat Commun. 2014 Nov;5(1):5324. doi: 10.1038/ncomms6324

61. Ramachandran A, Santiago JG. CRISPR Enzyme Kinetics for Molecular Diagnostics. Anal Chem. 2021 May;93(20):7456–64. doi: 10.1021/acs.analchem.1c00525

62. Huyke DA, Ramachandran A, Bashkirov VI, Kotseroglou EK, Kotseroglou T, Santiago JG. Enzyme Kinetics and Detector Sensitivity Determine Limits of Detection of Amplification-Free CRISPR-Cas12 and CRISPR-Cas13 Diagnostics. Anal Chem. 2022 Jul;94(27):9826–34. doi: 10.1021/acs.analchem.2c01670

63. Mergny JL, Sun JS, Rougee M, Montenay-Garestier T, Barcelo F, Chomilier J, et al. Sequence specificity in triple helix formation: experimental and theoretical studies of the effect of mismatches on triplex stability. Biochemistry. 1991 Oct;30(40):9791–8. DOI: 10.1021/bi00104a031